Published in final edited form as:
Neurobiol Aging. 2009 January ; 30(1): 103–111. doi:10.1016/j.neurobiolaging.2007.05.014.

Atrophy progression in semantic dementia with asymmetric temporal involvement: A tensor-based morphometry study

S.M. Brambati[a,b], **K.P. Rankin**[a], **J. Narvid**[a], **W.W. Seeley**[a], **D. Dean**[a], **H.J. Rosen**[a], **B.L. Miller**[a], **J. Ashburner**[c], and **M.L. Gorno-Tempini**[a,*]

[a]Memory Aging Center, UCSF Department of Neurology, San Francisco, CA, United States

[b]Università Vita-Salute San Raffaele, Milano, Italy

[c]Wellcome Department of Imaging Neuroscience, Functional Imaging Laboratory, London, UK

Abstract

We performed a longitudinal anatomical study to map the progression of gray matter atrophy in anatomically defined predominantly left (LTLV) and right (RTLV) temporal lobe variants of semantic dementia (SD). T1-weighted MRI scans were obtained at presentation and one-year follow-up from 13 LTLV, 6 RTLV, and 25 control subjects. Tensor-based morphometry (TBM) in SPM2 was applied to derive a voxel-wise estimation of regional tissue loss over time from the deformation field required to warp the follow-up scan to the presentation scan in each subject. When compared to controls, both LTLV and RTLV showed significant progression of gray matter atrophy not only within the temporal lobe most affected at presentation, but also in the controlateral temporal regions ($p < 0.05$ FWE corrected). In LTLV, significant progression of volume loss also involved the ventromedial frontal and the left anterior insular regions. These results identified the anatomic substrates of the previously reported clinical evolution of LTLV and RTLV into a unique 'merged' clinical syndrome characterized by semantic and behavioral deficits and bilateral temporal atrophy.

Keywords

Tensor-based morphometry; Semantic dementia; Temporal lobe; Progression of gray matter atrophy; Longitudinal study

1. Introduction

Semantic dementia (SD) is the variant of frontotemporal lobar degeneration (FTLD) characterized by progressive loss of conceptual knowledge (semantic memory) and anterior temporal lobe atrophy (Hodges et al., 1992; Neary et al., 1998). Asymmetrical hemispheric involvement is common in SD, with patients most often showing greater left than right temporal atrophy (Chan et al., 2001a,b; Galton et al., 2001; Gorno-Tempini et al., 2004a,b; Mummery et al., 2000; Rosen et al., 2002). The clinical syndrome associated with this pattern of predominantly left temporal involvement ('left temporal lobe variant', LTLV) corresponds to the classic description of SD, and is characterized by progressive naming, word comprehension and object recognition deficits (Hodges et al., 1992; Neary et al., 1998). On the other hand,

*Corresponding author at: UCSF Memory and Aging Center, 350 Parnassus Avenue, Suite 506, San Francisco, CA 94143, United States. Tel.: +1 415 476 1895; fax: +1 415 476 0213. *E-mail address:* marilu@memory.ucsf.edu (M.L. Gorno-Tempini)..

Conflicts of interest None.

when atrophy is greater in the right temporal lobe ('right temporal lobe variant', RTLV), patients often present with a different clinical syndrome where behavioral disturbances, such as personality changes, loss of empathy and compulsions, are prominent (Edwards-Lee et al., 1997; Gorno-Tempini et al., 2004a,b; Miller et al., 1993; Perry et al., 2001). Language deficits are less evident in RTLV at presentation, and semantic memory impairment is often limited to the categories of people, smells, or food (Evans et al., 1995; Gainotti et al., 2003; Gorno-Tempini et al., 2004a,b; Joubert et al., 2006; Thompson et al., 2004).

Later in the course of the disease, RTLV and LTLV become more difficult to distinguish. Seeley et al. (2005) performed a retrospective analysis of the clinical evolution of SD patients presenting with asymmetrical temporal atrophy. The study showed that, within three years of onset, the RTLV and LTLV clinical syndromes began to overlap. Specifically, whilst presenting symptoms progressed, LTLV patients also developed a behavioral syndrome, while RTLV cases also showed a more generalized semantic and language impairment. The anatomical basis of this progressive clinical merging of RTLV and LTLV has not yet been investigated.

Objective and automated mapping of tissue loss over time can be achieved using specifically designed neuroimaging MRI techniques, such as tensor-based morphometry (TBM) (Leow et al., 2006). In TBM volume changes are inferred from the non-linear deformation field required to warp two serial MRI scans. This technique has proven useful for tracking progression of atrophy in various neurodegenerative diseases (Chan et al., 2001a,b; Fox et al., 2000, 2001, 1999; Fox and Freeborough, 1997; Freeborough et al., 1996; Kipps et al., 2005; Leow et al., 2006; Studholme et al., 2001). A TBM-like approach has been applied to serial scans of classic SD patients and has shown progression of atrophy in the temporal lobes (Cardenas and Studholme, 2004; Whitwell et al., 2004), but longitudinal neuroimaging studies of patients with predominant right or left temporal atrophy are still lacking.

The aim of this longitudinal neuroimaging study was to identify patterns of regional atrophy progression in LTLV and RTLV in the first year following diagnosis. TBM, as implemented in the Statistical Parametric Mapping software (SPM2), was used to obtain and compare maps of gray matter contraction over time in LTLV and RTLV patients and controls. Based on previous clinical evidence, we hypothesize that, as disease progresses, atrophy changes will include the temporal lobe least affected at presentation and the ventromedial frontal regions.

2. Methods

2.1. Subjects

MR images were obtained at presentation (Time 1) and at one-year follow-up (Time 2) from 19 right-handed SD patients (mean age 62.1 ± 6.0 years, 12 males, 7 females) and 25 healthy controls (mean age 64.8 ± 6.9 years, 9 males, 16 females). All patients were evaluated at UCSF Memory and Aging Center by a team of clinicians with expertise in neurodegenerative diseases, including a behavioral neurologist, a neuropsychologist, a nurse, and a psychiatrist. Only cases for which a consensus diagnosis of SD (Neary et al., 1998) or normal cognition was reached were included in the study. Results from an automated volumetric analysis of the temporal lobes were used to designate subjects as LTLV or RTLV at Time 1.

All subjects or their caregivers provided written informed consent. The study was approved by the UCSF committee on human research.

2.2. Image acquisition

Presentation and one-year follow-up MRI scans were obtained on a 1.5 Tesla Magneton VISION system (Siemens Inc., Iselin, NJ) equipped with a standard quadrature head coil.

Structural MRI sequences included: (1) two-dimensional, fast low-angle shot (FLASH) MRI along three orthogonal directions; 3 mm thick slices with 15 slices in each direction to obtain scout views of the brain for positioning MRI slices; (2) a double spin echo sequence (TR/$[TE]_1/TE_2$ = 5000/20/80 ms) to obtain proton density and T2-weighted MRI; 51 contiguous axial slices (3 mm) covering the entire brain and angulate -10° from the anterior commissure (AC)- posterior commissure (PC) line; 1.0mm×1.25mm in-plane resolution; (3) volumetric magnetization prepared rapid gradient echo (MPRAGE)sequence (TR/TE/inversion time [TI] = 10/4/300 ms, flip angle = 15°) to obtain a T1-weighted image of the entire brain. The images were acquired with a coronal slice plane with in-plane pixel size of 1.0mm×1.0mm and slice thickness of 1.5 mm, with a matrix size of 256×192.

2.3. LTLV and RTLV group classification

2.3.1. Temporal lobe volume measurement methodology—Cross-sectional left and right temporal lobe volumes were calculated from the scan at presentation, in order to classify patients as LTLV and RTLV, and at one-year follow-up. Volumes were generated using the BRAINS2 software (Magnotta et al., 2002), which allows automated volume measurement of the major lobes based on their location within the standardized grid of Talairach and Tournoux. Processing of images included reorientation of each T1 weighted image to make the anterior-posterior axis parallel with the anterior commissure-posterior commissure (AC-PC) line, and identification of outer boundaries of the brain in order to warp the Talairach grid onto the brain. The T2 and proton density weighted images were then realigned to the T1 weighted image using an automated image registration program (Woods et al., 1992). A mask delineating brain versus non-brain tissue was created by first segmenting the brain into gray matter, white matter, and CSF compartments using the three coregistered images and a discriminant analysis method (Harris et al., 1999), and then generating the mask using an artificial neural network. Temporal volumes were calculated from all brain tissue (gray plus white matter) falling within the portions of the Talairach grid corresponding to temporal lobe (Woods et al., 1992). The volumes reported here were normalized to correct for differences in overall head size using total intracranial volume (gray matter, plus white matter plus CSF) derived from segmented images.

2.3.2. LTLV and RTLV patient sample—Temporal volumes for each patient were compared to controls, and *Z* scores were created individually for left and right temporal lobe. *Z* scores represented how many standard deviations each patient's temporal volumes were below the mean of the control group. They were calculated by subtracting the mean of temporal lobe volumes in the control group from each patient's temporal volume and then dividing the difference by the control group standard deviation. Patients were then classified as LTLV or RTLV at Time 1 based on which temporal lobe had greater negative *Z* scores. Thus, 13 SD patients were classified as LTLV (mean age 62.0 ± 6.3 years, nine males, four females) and six as RTLV (mean age 62.5 ± 5.7 years, three males, three females) (see Table 1). This is consistent with previous studies showing that LTLV is roughly three times more prevalent than RTLV (Seeley et al., 2005;Thompson et al., 2003). There was no significant difference between LTLV and RTLV for age, education, sex, and interval between MRI scans (Table 1). Although the mean time from disease onset to the presentation scan was longer in RTLV than in LTLV (RTLV: 5.7 ± 3.7 years, LTLV: 3.2 ± 1.1), the statistical comparison only showed a trend towards significance (T = -1.6, p = 0.17). Six patients included in this study have been previously described by Seeley et al. (2005). Despite the different tracing methodologies adopted by the two studies, patients were consistently classified as RTLV (n = 3) and LTLV (n = 3). RTLV showed greater atrophy than LTLV in both the most (*Z* score of right temporal lobe in RTLV versus left in LTLV) and the least (*Z* score of left temporal lobe in RTLV versus right in LTLV) damaged temporal lobes. Each patient showed a difference between temporal

lobe *Z* scores of at least 1.5 standard deviations at presentation. Both left and right temporal lobe volumes decreased over one year from diagnosis in the two variants of SD.

2.4. LTLV and RTLV neuropsychological assessment

Functional and neuropsychological screening was performed for diagnostic purposes both at the time of presentation (Time 1) and one-year follow-up (Time 2) in LTLV and RTLV patients, and at Time 1 in healthy aging controls. Clinical dementia rating (CDR) (Morris, 1993), mini mental state examination (MMSE) (Folstein et al., 1975) and neuropsychiatric inventory (NPI) (Srikanth et al., 2005) assessed general functional level and behavior. Standard tests evaluated language, working memory, visuospatial and executive functions.

Two-sample *t*-tests were used to assess cross-sectional neuropsychological differences between patients and controls and between RTLV and LTLV at Time 1 and Time 2. Paired sample *t*-tests were used to assess longitudinal changes between Time 1 and Time 2 within each patient group. Statistical analyses of neuropsychological data were performed using SAS statistical package (release 9.1, 2002, SAS Institute Inc., Cary, NC).

2.5. Whole-brain cross-sectional neuroimaging analysis at Time 1: voxel-based morphometry

VBM was applied to detect regional gray matter (GM) atrophy at Time 1 in LTLV and RTLV compared to controls across the whole brain. The VBM analysis included two steps: spatial preprocessing (normalization, segmentation, Jacobian modulation and smoothing) and statistical analysis. Both steps were implemented in the SPM2 software package (Wellcome Department of Imaging Neuroscience, London; http://www.fil.ion.ucl.ac.uk/spm) running on Matlab 6.5.1 (MathWorks, Natick, MA). MRI images were pre-processed using an optimized method for spatial normalization of gray matter, including creation of a study-specific template and *a priori* images (Good et al., 2001). Gray matter voxel values were multiplied by the Jacobian determinants derived from the spatial normalization step (Jacobian modulation) to preserve the initial volumes. Modulated gray matter images were then spatially smoothed with a 12 mm FWHM isotropic Gaussian kernel. The 12 mm kernel has been shown to minimize the risk of false positive findings (Salmond et al., 2002).

A ‘condition and covariates’ model was used and sex, age, and total intracranial volume at the Time 1 were entered into the statistical model as confounding variables. Gray matter volume differences between patients and controls were assessed using the general linear model (Friston et al., 1995a), and the significance of each effect was determined using the theory of Gaussian fields (Friston et al., 1995b). Specific contrasts were performed comparing gray matter volumes in the LTLV and RTLV groups versus controls. A level of significance of $p < 0.05$ corrected for multiple comparisons (SPM family wise error—FWE) was adopted.

2.6. Whole-brain longitudinal neuroimaging analysis: tensor-based morphometry

A whole-brain TBM analysis was used to map progression of regional gray matter (GM) atrophy over time in LTLV and RTLV compared to controls. Both spatial pre-processing and statistical analysis were implemented in SPM2. Details regarding TBM image pre-processing are described in previous studies (Brambati et al., 2007; Kipps et al., 2005)(Fig. 1). We applied a bias correction to the follow-up T1-weighted scan previously coregistered with the presentation image. A high-dimensional deformation field was then used to warp the corrected late image to match the early one within subject (Ashburner et al., 2000). The amount of volume change was quantified by taking the determinant of the gradient of deformation at a single-voxel level (Jacobian determinants). The following formula was applied to the segmented gray matter image obtained from the first scan (Ashburner and Friston, 2003) and the Jacobian determinant map: (Jacobian value - 1) × GM. The resulting product image represented a

measure of the gray matter specific volume change between the first and the second scan. Study-specific template and *a priori* images were created by averaging each subject's early and late normalized images. The normalization parameters were estimated by matching the customized gray matter template with the segmented gray matter image from the first scan. The normalization parameters were then applied to the product image (Ashburner and Friston, 1999). Normalized images were smoothed using a 12 mm isotropic Gaussian kernel. Finally, smoothed images were multiplied by an inclusive binary mask identifying only gray matter tissue. Main pre-processing steps are summarized in Fig. 1.

Normalized, smoothed maps of gray matter contraction over time for each subject were entered into the statistical analysis. A 'condition and covariates' model was used and sex, age, and total intracranial volume at the Time 2 were entered into the statistical model as confounding variables. Specific contrasts were performed comparing gray matter contraction in the LTLV and RTLV groups versus controls. A level of significance of $p < 0.05$ corrected for multiple comparisons (SPM family wise error—FWE) was adopted.

3. Results

3.1. LTLV and RTLV neuropsychological performance

At presentation, LTLV and RTLV patients showed comparable CDR and MMSE scores suggesting borderline functional status (see Table 1). Consistently with SD diagnosis, when compared to normal controls, both LTLV and RTLV showed deficits in language (phonemic and category fluency, and naming test) and behavior (Neuropsychiatric Inventory), in the context of fairly intact visuospatial (Modified Rey-Osterrieth Copy), working memory (Digit Backward) and executive (Modified Trials) abilities. LTLV revealed impaired comprehension of spoken single words as well (Auditory Word Recognition subtest of the Western Aphasia Battery).

When the scores of the two patients' groups at Time 1 were compared, no significant differences were observed in neuropsychological tests, but RTLV revealed greater behavioral symptoms.

Longitudinal analyses showed that semantic fluency significantly decreased in both LTLV and RTLV. Naming, single word comprehension and digit backward scores worsened in both RTLV and LTLV, but the result reached significance only in the larger LTLV group. Behavioral symptoms, as measure by the NPI, increased in RTLV.

3.2. Whole-brain voxel-based morphometry results: pattern of gray matter atrophy at Time 1

3.2.1. LTLV versus controls (Table 2 and Fig. 2A)—In LTLV patients at presentation, extensive gray matter volume loss was observed within the left temporal lobe, confirming the lobar volume measurements. Gray matter atrophy was mainly found in the anterior portion of the left temporal lobe, including the pole (BA 38), the middle (BA 21), inferior (20) and fusiform (BA 20/37) gyri. GM loss extended to the medial portion of the left temporal lobe, including the hippocampus/amygdala.

Less extensive gray matter atrophy was also observed in controlateral temporal regions, including the right inferior temporal (BA 20), fusiform (BA 20/37) and parahippocampal (BA 36) gyri, and the hippocampus/amygdala.

Outside the temporal lobes, tissue loss was observed in the left insula and caudate.

3.2.2. RTLV versus controls (Table 2 and Fig. 2B)—In RTLV patients at presentation, extensive gray matter volume loss was observed within the right temporal lobe, confirming the lobar volume measurements. Specifically, GM atrophy involved the right temporal pole (BA

38), the superior (BA 22), middle (BA 21) and inferior (BA 20) temporal and fusiform (BA 20/37) gyri. GM loss extended to the medial portion of the left temporal lobe, including the parahippocampal gyrus (BA 36), hippocampus/amygdala.

Gray matter atrophy was also observed in controlateral temporal regions, including the inferior temporal (BA 20) and fusiform (BA 20/37) gyri and in the hippocampus/amygdala.

Outside the temporal lobes, GM atrophy was observed within the right insula.

3.3. Whole-brain tensor-based morphometry results: gray matter atrophy progression

3.3.1. LTLV versus controls (Table 3 and Fig. 3)—In LTLV, over one year from initial diagnosis, significant gray matter contraction was found in the temporal lobe that was most affected at presentation (left), and also in the least affected (right). Specifically, within the left temporal lobe, significant gray matter (GM) contraction was observed in the temporal pole (BA 38), extending posteriorly in the fusiform (BA 20/37) and lingual (BA 37) gyri.

Within the right temporal lobe, the side least affected at clinical presentation in LTLV, significant volume loss was found in the temporal pole (BA 38), in the middle (BA 21) and inferior (BA 20) temporal gyri and, more posteriorly, in the fusiform gyrus (BA 20/37). In the medial portion of the temporal lobes, progressive GM contraction was observed bilaterally in the amygdala/hippocampus regions.

Outside of the temporal lobes, significant gray matter contractions were also found in the left anterior insula, bilateral ventromedial frontal cortex (BA 25/11), caudate and the right thalamus.

3.3.2. RTLV versus controls (Table 3 and Fig. 3B)—In RTLV, over one year from initial diagnosis, significant gray matter contraction was observed in the temporal lobe that was most affected at presentation (right), and also in the least affected (left).

Specifically, within the right temporal lobe, more affected at presentation, progressive atrophy over time was observed in the superior (BA 22) and middle temporal (BA 21) gyri.

Within the left temporal lobe, the side least affected at clinical presentation, significant volume loss was found in the temporal pole (BA 38), in the inferior temporal (BA 20) and fusiform (BA 20/37) gyri. In the left medial temporal lobe, progressive GM contraction was observed in the amygdala/hippocampus regions.

Outside of the temporal lobes, no region showed progression of atrophy in the RTLV group at a corrected level of significance. A trend of longitudinal change was observed in the right amygdala/hippocampus (x = 20, y = -15, z = -24, Z score = 3.1; $p < 0.001$ uncorrected) and bilaterally in the insula (x =-43, y =-18, z=5, Z score = 3.7; x = 33, y = 18, z=0, Z score = 3.4; $p < 0.001$ uncorrected) and ventromedial frontal cortex (x =-10, y = 14, z =-14, Z score = 4.8; x=8, y = 16, z = -12, Z score=4.5 $p < 0.001$ uncorrected).

3.3.3. Correlation analysis between changes in temporal lobe atrophy and cognitive scores—A correlation analysis was performed to test the hypothesis that the worsening of semantic and behavioral symptoms was associated with the progression of gray matter atrophy in the left and right temporal pole, respectively. Measures of semantic and behavioral deficit progression were derived by subtracting Time 1 from Time 2 scores in single word comprehension (Auditory Word Recognition subtest of the WAB), picture naming (Boston Naming Test—BNT) and from the Neuropsychiatric Inventory (NPI) scale. Values of gray matter atrophy progression were extracted from the left and in the right temporal poles

anatomically defined using the AAL brain atlas (Tzourio-Mazoyer et al., 2002) implemented in the WFU Pickatlas software (Maldjian et al., 2004; Maldjian et al., 2003).

The results showed that worsening of single word comprehension deficits significantly correlated with atrophy progression in the left ($R = 0.69$, $p < 0.05$), but not in the right ($R = -0.17$, $p = 0.65$) temporal pole. GM atrophy progression in either temporal pole did not reveal significant correlation with worsening of naming abilities or behavioral symptoms.

4. Discussion

We used tensor-based morphometry to map the progression of gray matter atrophy in patients with anatomically defined left (LTLV) or right (RTLV) temporal lobe variants of semantic dementia (SD) over a one-year period from initial diagnosis. In both variants, results showed gray matter contraction in the temporal lobe most affected at presentation, but also significant changes in the least affected side. This finding provides the anatomical substrate of the clinical overlap between the two syndromes as disease progresses (Seeley et al., 2005). A correlation analysis showed that changes in word-comprehension abilities correlated with the progression of gray matter atrophy in the left temporal pole.

The progressive loss of semantic memory typical of SD has been associated with predominantly left-sided temporal lobe degeneration (LTLV). Anomia and word comprehension deficits are usually the earliest and most severe clinical symptoms of a semantic memory breakdown (Seeley et al., 2005). The early clinical features of predominantly right temporal atrophy (RTLV) are more controversial. The term “semantic dementia” might not even apply in some early RTLV cases in which the predominant symptoms are behavioral abnormalities and face recognition deficits, in the context of relatively spared language abilities (Edwards-Lee et al., 1997; Evans et al., 1995; Gainotti et al., 2003; Gorno-Tempini et al., 2004a,b; Joubert et al., 2006; Joubert et al., 2003; Miller et al., 1993; Perry et al., 2001; Thompson et al., 2004). RTLV patients at this early stage rarely present at neurology specialty clinics. In these cases, the diagnosis of a neurodegenerative disease is often made later, when behavioral abnormalities become noticeable to caregivers and when language symptoms typical of left temporal degeneration also appear. At this stage of the disease, patients are often non-testable and non-compliant to examination, possibly explaining the rare reports of RTLV cases in the neurological literature. Conversely, LTLV patients are commonly diagnosed earlier, as the presenting language symptoms are soon noticed by patients and caregivers. However, as time passes, LTLV develop behavioral symptoms similar to those of RTLV, such as emotional detachment with loss of empathy. It has been proposed that the emergence of language symptoms in RTLV and of behavioral disturbances in LTLV may result from spreading of gray matter atrophy to the controlateral hemisphere (Seeley et al., 2005). Our results support this hypothesis by showing progression of atrophy in the controlateral hemisphere in both LTLV and RTLV. Furthermore, our correlation analysis showed that changes in single word comprehension abilities correlated with progression of gray matter atrophy in the left but not right temporal pole. This result confirms previous evidence from a cross-sectional VBM study that correlated object-based semantic abilities with atrophy in the left temporal pole (Mummery et al., 2000). The surprising lack of correlation between loss of naming abilities and progression of atrophy in the temporal poles, previously reported by Avants et al. (2005), can probably be ascribed to the fact that naming scores were already at floor at Time 1 (see Table 1). Our analysis showed that the worsening of behavioral symptoms, as assessed by the NPI, did not correlate with temporal pole volume loss over time. This finding could be explained by the fact that the NPI does not specifically assess the behavior abnormalities typically associated with RTLV and right temporal lobe function, such as loss empathy and personality changes (Rankin et al., 2006; Seeley et al., 2005). Further studies, involving larger groups of patients

and including objective measures of behavioral deficits typical of RTLV are necessary to identify the specific role of the right temporal poles in SD progression.

Progression of atrophy in LTLV also involved regions of the ventromedial frontal cortex, amygdalae/hippocampi region and left insula, which belong to a distributed network for control of emotional behavior (Ongur and Price, 2000). Accordingly, progressive atrophy in these areas could be associated with emergence of deficits in social functioning and feeding behavior manifested by LTLV in later stages of the disease (Seeley et al., 2005; Woolley, in press).

In both variants, the progression of atrophy relatively spares parietal, occipital and dorsal frontal brain regions in SD. This may explain the fairly intact visuospatial (Edwards-Lee et al., 1997) and working memory functions (Waltz et al., 1999) previously reported in SD and also observed in our sample (see Table 1).

TBM is a recently introduced technique that was successful at identifying patterns of atrophy progression typical of various neurodegenerative disorders (Brambati et al., 2007; Chan et al., 2001a,b; Fox et al., 2000, 2001, 1999; Fox and Freeborough, 1997; Freeborough et al., 1996; Kipps et al., 2005; Leow et al., 2006; Studholme et al., 2001), including classic SD (Cardenas and Studholme, 2004; Whitwell et al., 2004). Here, we showed that the automated, whole-brain TBM technique as implemented in SPM, could detect differential patterns of longitudinal gray matter atrophy in two variants of the same disease. These results suggest that this technique is useful tool in tracking of disease progression in neurodegenerative diseases.

Acknowledgments

The study was supported by the National Institute of Neurological Disorders and Stroke (R01 NS050915), the State of California (DHS 04-35516), the National Institute on Aging (P50 AG03006, P01 AG019724), the John Douglas French Alzheimer's Foundation, the McBean Foundation, the Sandler Foundation, the Alzheimer's Disease Research Center of California (03-75271 DHS/ADP/ARCC), the Larry Hill-blom Foundation (grant #2002/2F) and the Koret Foundation (grant 99-0102). We thank patients and their families for the time and effort they dedicate to our research.

References

Ashburner J, Andersson JL, Friston KJ. Image registration using a symmetric prior—in three dimensions. Hum. Brain Mapp 2000;9(4):212–225. [PubMed: 10770230]

Ashburner, J.; Friston, KJ. Image segmentation. In: Frackowiack, KJFRSJ.; Frith, C.; Dolan, R.; Friston, KJ.; Price, CJ.; Zeki, S.; Ashburner, J.; Penny, WD., editors. Human Brain Function. Academic Press; 2003.

Ashburner J, Friston KJ. Nonlinear spatial normalization using basis functions. Hum. Brain Mapp 1999;7 (4):254–266. [PubMed: 10408769]

Avants B, Grossman M, Gee JC. The correlation of cognitive decline with frontotemporal dementia induced annualized gray matter loss using diffeomorphic morphometry. Alzheimer Dis. Assoc. Disord 2005;19(Suppl 1):S25–S28. [PubMed: 16317254]

Brambati SM, Renda NC, Rankin KP, Rosen H, Seeley WW, Ashburner J, Miller BL, Gorno-Tempini ML. A tensor based morphometry study of longitudinal gray matter contraction in FTD. NeuroImage 2007;35(3):998–1003. [PubMed: 17350290]

Cardenas V, Studholme C. Co-analysis of maps of atrophy rate and atrophy state in neurodegeneration. MICCAI 2004:680–687.

Chan D, Fox NC, Jenkins R, Scahill RI, Crum WR, Rossor MN. Rates of global and regional cerebral atrophy in AD and frontotemporal dementia. Neurology 2001a;57(10):1756–1763. [PubMed: 11723259]

Chan D, Fox NC, Scahill RI, Crum WR, Whitwell JL, Leschziner G, Rossor AM, Stevens JM, Cipolotti L, Rossor MN. Patterns of temporal lobe atrophy in semantic dementia and Alzheimer's disease. Ann. Neurol 2001b;49(4):433–442. [PubMed: 11310620]

Edwards-Lee T, Miller BL, Benson DF, Cummings JL, Russell GL, Boone K, Mena I. The temporal variant of frontotemporal dementia. Brain J. Neurol 1997;120(Pt 6):1027–1040.

Evans JJ, Heggs AJ, Antoun N, Hodges JR. Progressive prosopagnosia associated with selective right temporal lobe atrophy. A new syndrome? Brain J. Neurol 1995;118(Pt 1):1–13.

Folstein MF, Folstein SE, McHugh PR. "Mini-mental state": a practical method for grading the cognitive state of patients for the clinician. J. Psychiat. Res 1975;12(3):189–198. [PubMed: 1202204]

Fox NC, Cousens S, Scahill R, Harvey RJ, Rossor MN. Using serial registered brain magnetic resonance imaging to measure disease progression in Alzheimer disease: power calculations and estimates of sample size to detect treatment effects. Arch. Neurol 2000;57(3):339–344. [PubMed: 10714659]

Fox NC, Crum WR, Scahill RI, Stevens JM, Janssen JC, Rossor MN. Imaging of onset and progression of Alzheimer's disease with voxel-compression mapping of serial magnetic resonance images. LANCET 2001;358(9277):201–205. [PubMed: 11476837]

Fox NC, Freeborough PA. Brain atrophy progression measured from registered serial MRI: validation and application to Alzheimer's disease. J. Magn. Res. Imaging 1997;7(6):1069–1075.

Fox NC, Scahill RI, Crum WR, Rossor MN. Correlation between rates of brain atrophy and cognitive decline in AD. Neurology 1999;52(8):1687–1689. [PubMed: 10331700]

Freeborough PA, Woods RP, Fox NC. Accurate registration of serial 3D MR brain images and its application to visualizing change in neurodegenerative disorders. J. Comput. Assist. Tomo 1996;20 (6):1012–1022.

Friston KJ, Holmes A, Poline J-B, Price CJ, Frith CD. Detecting activations in PET and fMRI: levels of inference and power. NeuroImage 1995a;40:223–235.

Friston KJ, Holmes AP, Worsley KJ, Poline J-B, Frith CD, Frackowiak RSJ. Statistical parametric maps in functional imaging: a general linear approach. Hum. Brain Mapp 1995b;2:189–210.

Gainotti G, Barbier A, Marra C. Slowly progressive defect in recognition of familiar people in a patient with right anterior temporal atrophy. Brain J. Neurol 2003;126(Part 4):792–803.

Galton CJ, Patterson K, Graham K, Lambon-Ralph MA, Williams G, Antoun N, Sahakian BJ, Hodges JR. Differing patterns of temporal atrophy in Alzheimer's disease and semantic dementia. Neurology 2001;57(2):216–225. [PubMed: 11468305]

Good CD, Johnsrude IS, Ashburner J, Henson RN, Friston KJ, Frackowiak RS. A voxel-based morphometric study of ageing in 465 normal adult human brains. NeuroImage 2001;14(1 Part 1): 21–36. [PubMed: 11525331]

Gorno-Tempini ML, Dronkers NF, Rankin KP, Ogar JM, Phengrasamy L, Rosen HJ, Johnson JK, Weiner MW, Miller BL. Cognition and anatomy in three variants of primary progressive aphasia. Ann. Neurol 2004a;55(3):335–346. [PubMed: 14991811]

Gorno-Tempini ML, Rankin KP, Woolley JD, Rosen HJ, Phengrasamy L, Miller BL. Cognitive and behavioral profile in a case of right anterior temporal lobe neurodegeneration. Cortex 2004b;40:631–644. [PubMed: 15505973]

Harris G, Andreasen NC, Cizadlo T, Bailey JM, Bockholt HJ, Magnotta VA, Arndt S. Improving tissue classification in MRI: a three-dimensional multispectral discriminant analysis method with automated training class selection. J. Comput. Assist. Tomo 1999;23(1):144–154.

Hodges JR, Patterson K, Oxbury S, Funnell E. Semantic dementia. Progressive fluent aphasia with temporal lobe atrophy. Brain J. Neurol 1992;115(Pt 6):1783–1806.

Joubert S, Felician O, Barbeau E, Ranjeva JP, Christophe M, Didic M, Poncet M, Ceccaldi M. The right temporal lobe variant of frontotemporal dementia: cognitive and neuroanatomical profile of three patients. J. Neurol. 2006

Joubert S, Felician O, Barbeau E, Sontheimer A, Barton JJ, Ceccaldi M, Poncet M. Impaired configurational processing in a case of progressive prosopagnosia associated with predominant right temporal lobe atrophy. Brain; J. Neurol 2003;126(Part 11):2537–2550.

Kipps CM, Duggins AJ, Mahant N, Gomes L, Ashburner J, McCusker EA. Progression of structural neuropathology in pre-clinical Huntington's disease: a tensor based morphometry study. J. Neurol. Neurosurg. Psychiat 2005;76(5):650–655. [PubMed: 15834021]

Leow AD, Klunder AD, Jack J, Clifford R, Toga AW, Dale AM, Bernstein MA, Britson PJ, Gunter JL, Ward CP. Longitudinal stability of MRI for mapping brain change using tensor-based morphometry. Neuroimage 2006;31(2):627–640. [PubMed: 16480900]

Magnotta VA, Harris G, Andreasen NC, O'Leary DS, Yuh WTC, Heckel D. Structural MR image processing using the BRAINS2 toolbox. Comput. Med. Imaging Graph.: Off. J. Comput. Med. Imaging Soc 2002;26(4):251–264.

Maldjian JA, Laurienti PJ, Burdette JH. Precentral gyrus discrepancy in electronic versions of the Talairach atlas. Neuroimage 2004;21(1):450–455. [PubMed: 14741682]

Maldjian JA, Laurienti PJ, Kraft RA, Burdette JH. An automated method for neuroanatomic and cytoarchitectonic atlas-based interrogation of fMRI data sets. Neuroimage 2003;19(3):1233–1239. [PubMed: 12880848]

Miller BL, Chang L, Mena I, Boone K, Lesser IM. Progressive right frontotemporal degeneration: clinical, neuropsychological and SPECT characteristics. Dementia 1993;4(34):204–213. [PubMed: 8401793]

Morris JC. The clinical dementia rating (CDR): current version and scoring rules. Neurology 1993;43 (11):2412–2414. [PubMed: 8232972]

Mummery CJ, Patterson K, Price CJ, Ashburner J, Frackowiak RS, Hodges JR. A voxel-based morphometry study of semantic dementia: relationship between temporal lobe atrophy and semantic memory. Ann. Neurol 2000;47(1):36–45. [PubMed: 10632099]

Neary D, Snowden JS, Gustafson L, Passant U, Stuss D, Black S, Freedman M, Kertesz A, Robert PH, Albert M, Boone K, Miller BL, Cummings J, Benson DF. Frontotemporal lobar degeneration: a consensus on clinical diagnostic criteria. Neurology 1998;51(6):1546–1554. [PubMed: 9855500]

Ongur D, Price JL. The organization of networks within the orbital and medial prefrontal cortex of rats, monkeys and humans. Cereb. Cortex 2000;10(3):206–219. [PubMed: 10731217]

Perry RJ, Rosen HR, Kramer JH, Beer JS, Levenson RL, Miller BL. Hemispheric dominance for emotions, empathy and social behaviour: evidence from right and left handers with frontotemporal dementia. Neurocase Case Studies Neuropsychol. Neuropsychiat. Behav. Neurol 2001;7(2):145–160.

Rankin KP, Gorno-Tempini ML, Allison SC, Stanley CM, Glenn S, Weiner MW, Miller BL. Structural anatomy of empathy in neurodegenerative disease. Brain 2006;129(Pt 11):2945–2956. [PubMed: 17008334]

Rosen HJ, Gorno-Tempini ML, Goldman WP, Perry RJ, Schuff N, Weiner M, Feiwell R, Kramer JH, Miller BL. Patterns of brain atrophy in frontotemporal dementia and semantic dementia. Neurology 2002;58(2):198–208. [PubMed: 11805245]

Salmond CH, Ashburner J, Vargha-Khadem F, Connelly A, Gadian DG, Friston KJ. Distributional assumptions in voxel-based morphometry. Neuroimage 2002;17(2):1027–1030. [PubMed: 12377176]

Seeley WW, Bauer AM, Miller BL, Gorno-Tempini ML, Kramer JH, Weiner M, Rosen HJ. The natural history of temporal variant frontotemporal dementia. Neurology 2005;64(8):1384–1390. [PubMed: 15851728]

Srikanth S, Nagaraja AV, Ratnavalli E. Neuropsychiatric symptoms in dementia-frequency, relationship to dementia severity and comparison in Alzheimer's disease, vascular dementia and frontotemporal dementia. J. Neurol. Sci 2005;236(12):43–48. [PubMed: 15964021]

Studholme C, Cardenas V, Schuff N, Rosen H, Miller B, Weiner M. Detecting spacially consistent structural differences in Alzheimer's and frontotemporal dementia using deformation morphometry. MICCAI 2001:41–48.

Thompson SA, Graham KS, Williams G, Patterson K, Kapur N, Hodges JR. Dissociating person-specific from general semantic knowledge: roles of the left and right temporal lobes. Neuropsychologia 2004;42(3):359–370. [PubMed: 14670574]

Thompson SA, Patterson K, Hodges JR. Left/right asymmetry of atrophy in semantic dementia: behavioral-cognitive implications. Neurology 2003;61(9):1196–1203. [PubMed: 14610120]

Tzourio-Mazoyer N, Landeau B, Papathanassiou D, Crivello F, Etard O, Delcroix N, Mazoyer B, Joliot M. Automated anatomical labeling of activations in SPM using a macroscopic anatomical parcellation of the MNI MRI single-subject brain. Neuroimage 2002;15(1):273–289. [PubMed: 11771995]

Waltz JA, Knowlton BJ, Holyoak KJ, Boone K, Mishkin FS, de Menezes Santos M, Thomas CR, Miller BL. A system for relational reasoning in human prefrontal cortex. Psychol. Sci 1999;10:119–125.

Whitwell JL, Anderson VM, Scahill RI, Rossor MN, Fox NC. Longitudinal patterns of regional change on volumetric MRI in frontotemporal lobar degeneration. Dement. Geriatr. Cogn. Disord 2004;17 (4):307–310. [PubMed: 15178942]

Woods RP, Cherry SR, Mazziotta JC. Rapid automated algorithm for aligning and reslicing PET images. J. Comput. Assist. Tomo 1992;16(4):620–633.

Woolley JD, Gorno-Tempini ML, Seeley WW, Rankin KP, Lee SS, Matthews B, Miller BL. Compulsive eating is associated with right orbitofrontal-insular-striatal circuit atrophy in frontotemporal dementia. Neurology. in press

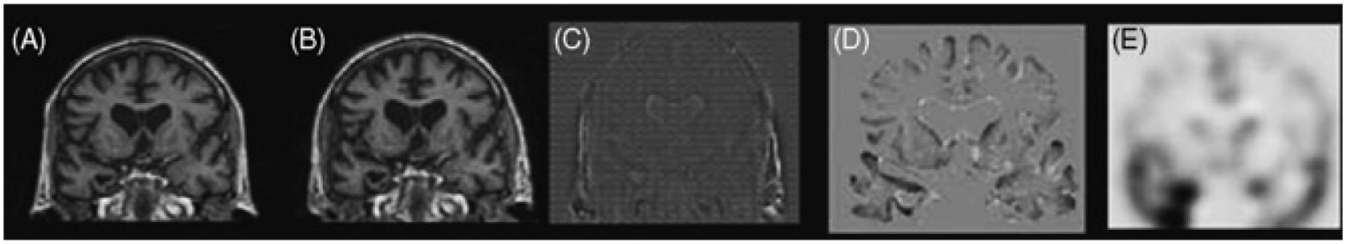

Fig. 1.

Example of main TBM pre-processing steps in a LTLV patient. (A) Presentation scan; (B) 1-year follow-up scan coregistered with the presentation scan; (C) Jacobian determinant map representing voxels of tissue expansion (voxel Jacobian value greater than 1) or contraction (voxel Jacobian value less than 1) from follow-up to presentation scan. Jacobian determinants were estimated by warping together the images A and B; (D) image representing gray matter volume changes between scans A and B. It was obtained by multiplying gray matter segment of the presentation scan with (Jacobian minus 1) values; (E) image D after normalization and smoothing process.

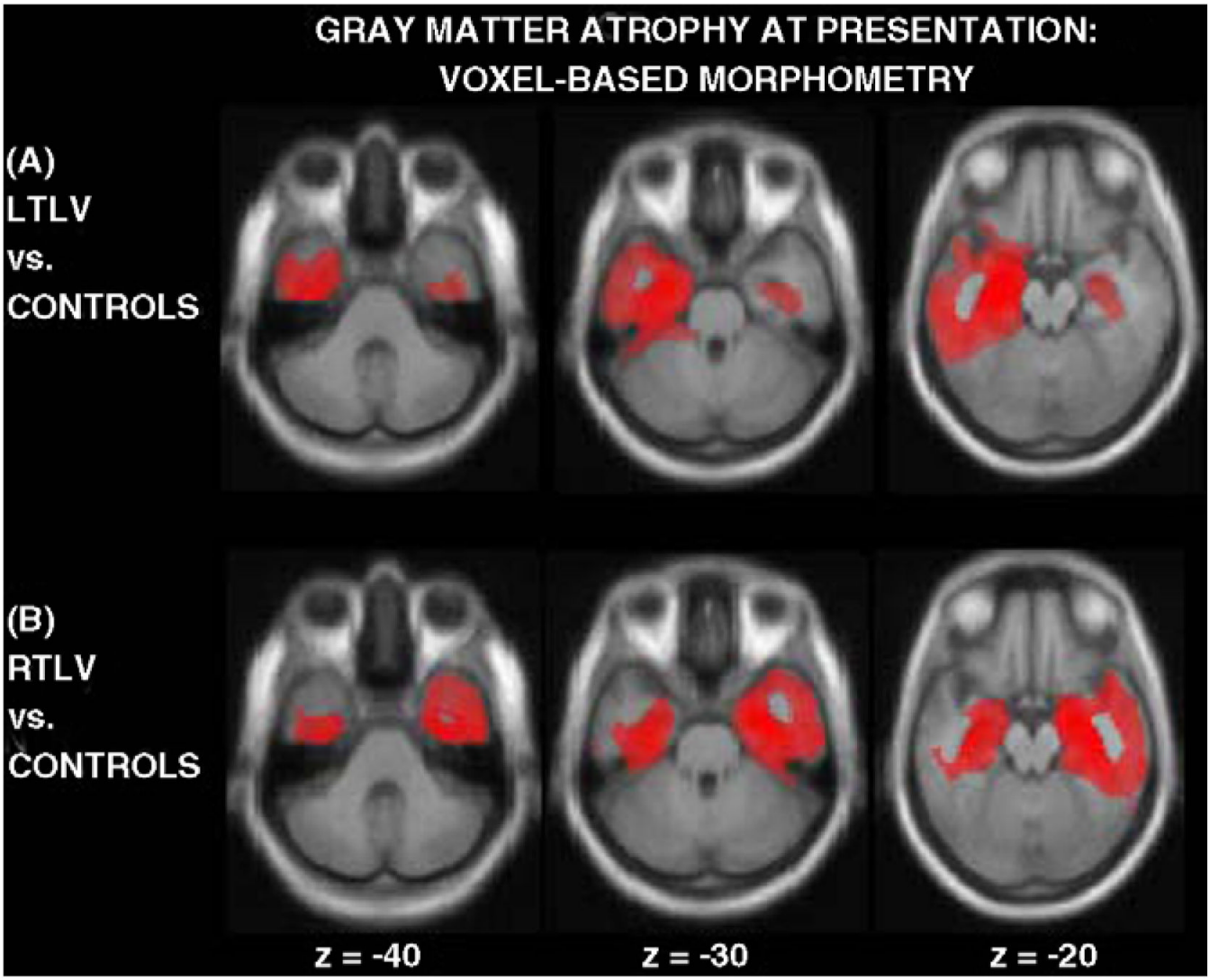

Fig. 2.

Whole-brain VBM analysis showing patterns of temporal gray matter atrophy in LTLV (A) and RTLV (B) patients compared with controls. Statistical maps are displayed on sections of the study-specific template used for normalization. The threshold for display is $p < 0.05$ corrected for multiple comparisons (SPM family-wise error—FWE). For display purpose, the result maps were multiplied by a binary inclusive mask derived by the GM a priori image.

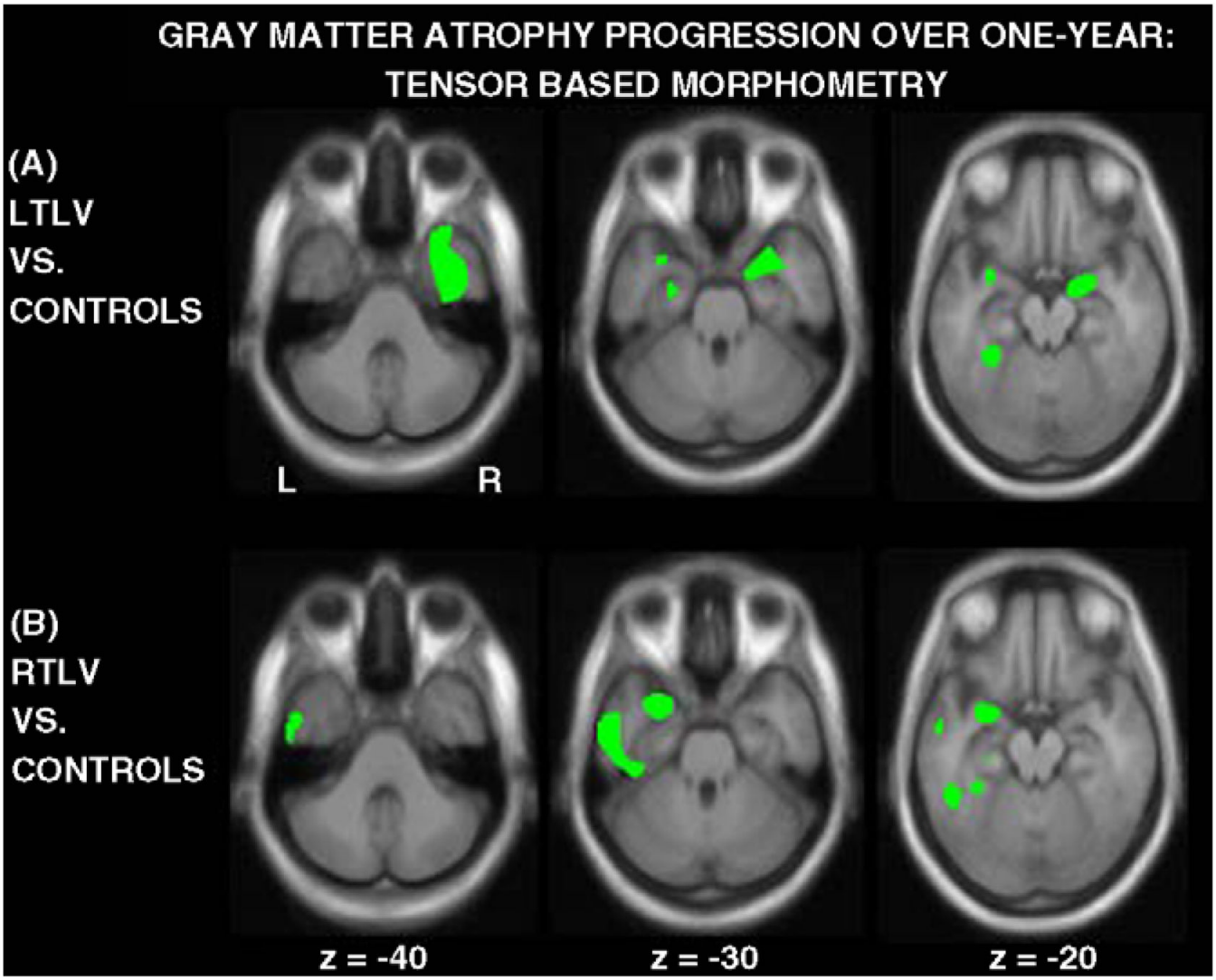

Fig. 3.

Whole-brain TBM analysis showing patterns of GM atrophy progression in LTLV patients versus controls (A) and RTLV patients versus controls (B) over 1 year after diagnosis. Statistical maps are displayed on sections of the study-specific template used for normalization. The threshold for display is $p < 0.05$ corrected for multiple comparisons (SPM family-wise error—FWE).

Table 1

Temporal volume Z scores, demographics and neuropsychological screening in LTLV and RTLV at Time 1 and Time 2 and in normal controls (NC) at Time 1

	LTLV		RTLV		NC
	Time 1	**Time 2**	**Time 1**	**Time 2**	**Time 1**
Temporal volume Z scores					
Left temporal volume Z score	-4.2 (1.5)	***-5.2 (1.4)***	-2.6 (1.1)§	***-3.6 (0.7)***§	-
Right temporal volume Z score	-1.7(1.7)	***-3.0 (2.2)***	-7.0 (1.6)§	***-8.2 (1.3)***§	-
Demographics					
Age	62.0 (6.3)	63.1 (6.3)	62.5 (5.8)	63.5 (5.8)	64.8 (6.9)
Education	16.6 (2.7)	-	14.5 (6.1)	-	17.0 (1.8)
Sex (M/F)	9/4	-	3/3	-	9/16
Years between disease onset and Time 1 scan	3.2 (1.1)	-	5.7 (3.7)	-	-
Months between MRI scans	12.0 (2.6)	-	12.4 (2.9)	-	11.3 (2.1)
Functional and cognitive status					
MMSE	22.0 (6.9)$^{\circ}$	21.2 (7.0)$^{\circ}$	27.0 (2.6)	***21.8 (3.4)***$^{\circ}$	29.6 (0.8)
CDR total	0.4 (0.3)$^{\circ}$	***0.5 (0.0)***$^{\circ}$	0.5 (0.0)$^{\circ}$	***1.0 (0.0)***$^{\circ}$	0.0 (0.2)
CDR box scores	1.9 (1.6)$^{\circ}$	***3.3 (3.2)***$^{\circ}$	3.0 (1.5)$^{\circ}$	***6.5 (0.5)***$^{\circ\,\S}$	0.1 (0.4)
Boston naming test (max =15)	3.9 (3.5)$^{\circ}$	***1.7 (1.8)***$^{\circ}$	5.0 (4.0)$^{\circ}$	2.0 (1.0)$^{\circ}$	14.7 (0.7)
WAB auditory word recognition (max = 60)	47.8 (13.8)$^{\circ}$	***36.2 (20.9)***$^{\circ}$	58.0 (2.0)	52.0 (6.2)$^{\circ}$	60.0 (0.0)
D-word verbal fluency (# words/min)	6.5 (4.5)$^{\circ}$	5.1 (3.8)$^{\circ}$	7.6 (1.8)$^{\circ}$	5.2 (2.9)$^{\circ}$	17.2 (5.7)
Animal fluency (# words/min)	5.9 (2.8)$^{\circ}$	***4.3 (2.2)***$^{\circ}$	7.0 (4.9)$^{\circ}$	***4.0 (2.9)***$^{\circ}$	23.3 (5.8)
Modified Rey-Osterrieth Copy (max = 17)	16.4 (0.9)	16.5 (0.7)	15.2 (1.5)	15.6 (1.5)	16.1 (1.1)
Modified trails (# correct items)	12.6 (4.0)	12.8 (3.8)	14.0 (0.0)	10.8 (6.6)	14.0 (0.0)
Digit backward	4.8 (1.0)	***4.4 (0.9)***$^{\circ}$	5.8 (0.5)§	5.3 (1.5)	5.7 (1.2)
NPI Scale-Total Score	12.7 (5.0)*	18.0 (6.0)*	20.3 (2.5)$^{*\,\S}$	***50.3 (7.7)***$^{*\,\S}$	-

Scores are reported as mean raw score (standard deviation). Means and standard deviations were obtained only from patients evaluated at both time points. Cross-sectional analyses

Abbreviations: MMSE: mini mental state examination; CDR: clinical dementia rating; NPI: neuropsychiatric inventory; WAB: western aphasia battery.

$^{\circ}$ $p < 0.05$ vs. NC (two-sample *t*-test)

§ $p < 0.05$ vs. LTLV at the same time point (two-sample *t*-test)

* impaired performance according to current norms (scores in NC not available). Longitudinal analyses: bold and italics: $p < 0.05$ in Time 1 vs. Time 2 (paired *t*-test).

Table 2

Voxel-based morphometry results

Brain regions atrophic at Time 1 (brodmann area)		LTLV (left temporal lobe variant)				RTLV (right temporal lobe variant)			
		x	*y*	*z*	Z score	*x*	*y*	*z*	Z score
Left temporal lobe									
Temporal pole (38)		-39	16	-28	6.5				-
		-46	12	-15	5.7				-
Middle temporal gyrus (21)		-48	-13	-13	5.6				-
		-55	3	-31	5.3				-
Inferior temporal gyrus (20)		-44	-32	-24	7.4	-45	-31	-22	5.5
		-57	-2	-32	5.3				-
Fusiform gyrus (20/37)		-34	-15	-36	7.7	-32	-16	-37	6.8
Amygdala/hippocampus		-27	-16	-20	7.8	-23	-12	-16	6.1
		-21	-9	-13	7.7				-
Right temporal lobe									
Temporal pole (38)					-	46	7	-21	5.7
Superior temporal gyrus (22)					-	46	2	-19	5.7
Middle temporal gyrus (21)					-	49	-22	-12	6.1
					-	54	-24	-27	5.6
Inferior temporal gyrus (20)		44	-13	-43	5.3	48	12	-41	6.4
					-	47	-17	-12	5.9
					-	55	-26	-24	5.4
Fusiform gyrus (20/37)		39	-17	-28	5.1	38	-18	-23	7.2
					-	35	-3	-40	5.9
Parahippocampal gyrus (36)		29	-11	-27	5	27	-26	-28	7.4
Amygdala/hippocampus		26	-12	-17	5.2	20	-10	-13	7.4
Basal ganglia									
Caudate	L	-8	13	8	5.1				-
Insula	L	-33	-9	18	5.9				-
	R				-	35	1	15	5.5

Regions showing gray matter atrophy at presentation in patients with anatomically defined left (LTLV) and right (RTLV) temporal lobe variant of SD compared to controls at a threshold of $p < 0.05$ corrected for multiple comparisons (SPM family-wise error-FWE).

Table 3

Tensor-based morphometry results

Brain regions that show progression of atrophy (brodmann area)		LTLV (left temporal lobe variant)				RTLV (right temporal lobe variant)			
		x	*y*	*z*	Z score	*x*	*y*	*z*	Z score
Left temporal lobe									
Temporal pole (38)		-34	6	-27	6.5	-32	5	-27	7.2
Inferior temporal gyrus (20)					-	-56	-10	-28	6.3
					-	-45	-41	-23	6.2
Fusiform gyrus (20/37)		-33	-38	-24	6.4	-38	-37	-25	6.2
					-	-29	-43	-15	5.7
Lingual gyrus (37)		-17	-44	-1	6.0				-
Amygdala/hippocampus		-30	-1	-14	5.9	-29	-2	-16	6.4
						-19	-43	-2	6.7
Right temporal lobe									
Temporal pole (38)		32	21	-35	5.7				-
		55	6	-13	5.3				-
Superior temporal gyrus (22)					-	58	-10	-1	5.0
Middle temporal gyrus (21)		57	-4	-24	5.3				-
					-	61	-30	-14	6.0
Inferior temporal gyrus (20)		40	0	-37	6.5				-
Fusiform gyrus (20/37)		25	-27	-26	5.3				-
Amygdala/hippocampus		19	-4	-22	6.2				-
		32	4	-32	6.1				-
Medial frontal lobe									
Ventromedial frontal cortex (25/11)	L	-8	16	-13	6.2				-
	R	8	16	-12	5.2				-
Basal ganglia									
Caudate	L	-17	14	6	6.3				-
	R	19	13	9	6.0				-
Thalamus	R	15	-8	8	5.6				-
Anterior insula	L	-27	13	-14	5.6				-

Regions showing progressive gray matter contraction in patients with anatomically defined left (LTLV) and right (RTLV) temporal lobe variant of SD compared to controls at a threshold of $p < 0.05$ corrected for multiple comparisons (SPM family-wise error-FWE).